

Prediction of the thermodynamics of protein unfolding: The helix-coil transition of poly(L-alanine)

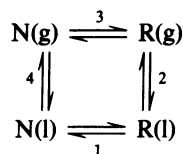
TATSUO OOI* AND MOTOHISA OOBATAKE†

*Kyoto Women's University, 35 Kitahiyoshi-cho, Imakumano, Higashiyama-ku, Kyoto 605, Japan; and †Protein Engineering Research Institute 6-2-3, Furuedai, Suita, Osaka 565, Japan

Communicated by Robert L. Baldwin, December 10, 1990

ABSTRACT The method given earlier for predicting the thermodynamics of protein unfolding from the x-ray structure of a protein is applied here to the poly(L-alanine) helix. First, the fitting parameters derived earlier from a data base of 10 proteins were used to predict the unfolding thermodynamics of 4 other proteins. The agreement between the observed and predicted values is comparable to that found for the 10 proteins studied initially. Next, the temperature dependences of the Gibbs energy and enthalpy changes for unfolding of bacteriophage T4 lysozyme were predicted and compared with data in the literature. The predicted and observed temperature dependences are similar and the predicted results indicate that cold denaturation should be observed at low temperatures, as observed recently for a T4 lysozyme mutant. The fitting parameters derived from thermodynamic data for protein unfolding and for hydration of model compounds were used to predict the unfolding thermodynamics of the poly(L-alanine) helix. The results predict that helix formation is enthalpy-driven, and the predicted enthalpy change for unfolding (0.86 kcal per mol per residue) is close to the value found in a recent calorimetric study of a 50-residue alanine-rich helix.

A method has been given recently for computing the effect of the interaction between a protein and water on the thermodynamics of protein unfolding (1-5). With the dry protein as a reference state, the method computes the thermodynamics of dehydration of both the native and unfolded forms of the protein by using fitting parameters derived from model compound data (1-3). The assumption is made that each atomic group interacts with water in proportion to its water-accessible surface area (ASA) in the protein structure. The atomic groups in the protein are divided into seven classes and thermodynamic data for the transfer of model compounds from gas phase into aqueous solution (6) are used to obtain the fitting parameters (1). The method can be understood by considering the following cycle.



N is the native protein and R is the unfolded random chain; g is the gas phase and l is the liquid phase (aqueous solution). Going counterclockwise around the cycle from N(l), step 1 is unfolding in aqueous solution, step 2 is dehydration of R(l), step 3 is the hypothetical process of folding the dry protein *in vacuo*, and step 4 is hydration of N(g). Experimental data for protein unfolding in aqueous solution are used for step 1. Thermodynamic data for hydration of model compounds are

used to compute the thermodynamics of steps 2 and 4 as explained above (see *Methods*).

Then enthalpy and entropy changes (ΔH and ΔS) associated with the hypothetical process of unfolding or refolding the dry protein (step 3) can be computed from the cycle. The signs of the steps below refer to unfolding and to dehydration.

$$\Delta H_3 = \Delta H_1 + \Delta H_2 - \Delta H_4$$

$$\Delta S_3 = \Delta S_1 + \Delta S_2 - \Delta S_4. \quad [1]$$

It may seem pointless to compute thermodynamic changes for a hypothetical process, unfolding a dry protein *in vacuo*, but the results have been used to provide a data base and then to obtain fitting parameters for step 3 (3). With these parameters and with the earlier parameters for computing the thermodynamics of hydration (1), the thermodynamics of unfolding in aqueous solution can be predicted for a protein from its x-ray structure.

This new method of analyzing the effect of protein hydration on the thermodynamics of protein unfolding differs in two basic respects from older methods: (i) it treats the interaction with water of both polar and nonpolar groups and (ii) it avoids using any nonpolar solvent as a reference state, and thus it avoids modeling the protein interior as an organic liquid. By including polar as well as nonpolar groups, the method is able to take into account the burial of polar groups, such as peptide NH and CO groups, during folding.

Older methods of analyzing protein hydration and its effect on the thermodynamics of protein unfolding focused on the nonpolar groups and their tendency to escape from water and to be buried in the interior during protein folding (7, 8). This tendency, which has been referred to as "the hydrophobic effect" or "the hydrophobic interaction," has been modeled (7, 8) by the transfer of hydrocarbon molecules from aqueous solution to a nonpolar solvent. This transfer reaction is assumed to be similar to the transfer of a hydrocarbon side chain in an unfolded protein from aqueous solution into the protein interior through folding. At present it is controversial whether it is better to use a highly nonpolar solvent such as cyclohexane or a more polar solvent such as water-saturated 1-octanol as the reference nonpolar liquid in the transfer of model compounds. Whereas the earlier methods (7, 8) have been successful in demonstrating the importance of the hydrophobic interaction as a major source of Gibbs energy driving protein folding, they have not been able to predict quantitatively the effect of protein hydration on the thermodynamics of unfolding.

Our present method has been found to give fairly successful prediction. The accuracy of prediction is limited by the fact that ΔH and ΔS of unfolding must each be computed as a difference between two large numbers (see below). The difference between ΔH_2 and ΔH_4 represents the contribution

of dehydration to unfolding. Thus, if ΔH_1 and ΔH_2 are denoted as ΔH^u and ΔS^u , for unfolding in aqueous solution, then each can be written as a sum of two terms.

$$\begin{aligned}\Delta H^u &= \Delta H_h^u + \Delta H_c^u \\ \Delta S^u &= \Delta S_h^u + \Delta S_c^u.\end{aligned}\quad [1']$$

The letter h (hydration) refers to the difference of steps 2 and 4 and the letter c (chain unfolding) refers to step 3.

In this way, a data base was obtained for step 3, using data for the thermodynamics of protein unfolding in aqueous solution (step 1) and the x-ray structure of the protein (for N) plus computer-generated random-chain structure (for R) to subtract the effect of dehydration (steps 2 and 4). Then fitting parameters were derived for step 3 from a data base of 10 proteins (3), again by assuming that ΔH_c^u and ΔS_c^u can be represented as a sum of products of ASAs multiplied by the fitting parameters for seven classes of atomic groups (see *Methods*).

The basic assumptions in this method are that steps 2, 3, and 4 can be represented by a formalism involving ASAs and thermodynamics of group transfer and that specific interactions can be neglected. In particular, the method does not explicitly take into account electrostatic interactions, which are evident in pH-dependent and salt-dependent effects. It is important, then, to choose problems for study by this method in which specific interactions can safely be neglected. The two problems studied here are unfolding of the L-alanine helix, which is electrically neutral, and the temperature dependence of the unfolding thermodynamics of bacteriophage T4 lysozyme. The temperature dependence of protein stability is governed chiefly by the hydrophobic interaction (9–13) and it is of interest to find out whether the new method predicts the existence of cold denaturation, which has been observed for myoglobin (14) and for a mutant of T4 lysozyme (15).

METHODS

Interaction Between the Protein and Water. An extensive compilation of Gibbs energy, enthalpy, and heat capacity changes for the transfer of model compounds from the gas phase to aqueous solution has been given (5). Some of these compounds are solids or liquids, and appropriate corrections for the thermodynamics of sublimation or vaporization have been made. Model compounds containing atomic groups found in proteins have been used (1) to derive best-fit parameters for representing the thermodynamic data as sums of products of the ASA of a particular group i times the appropriate hydration parameter g_{ih} , h_{ih} , s_{ih} , or c_{ih} for Gibbs energy, enthalpy, entropy, or heat capacity, respectively.

$$\begin{aligned}\Delta G_h &= \sum g_{ih} \Delta ASA_i \\ \Delta H_h &= \sum h_{ih} \Delta ASA_i \\ \Delta S_h &= \sum s_{ih} \Delta ASA_i \\ \Delta C_{p,h} &= \sum c_{ih} \Delta ASA_i.\end{aligned}\quad [2]$$

The seven kinds of atomic groups are hydrocarbon groups (including methyl and methylene groups), aromatic carbons, hydroxyl groups, amide and amine groups, carboxyl carbons, carboxyl oxygens, and sulfur-containing groups. The algorithm of Shrake and Rupley (16) was used to find the ASA of each group in the protein. Eqs. 2 apply to both the native (N) and the unfolded (R) form of the protein. The parameters g_{ih} , h_{ih} , and c_{ih} are given in ref. 1 and the parameters s_{ih} are easily

derived from g_{ih} and h_{ih} according to the thermodynamic relation.

The Reference States: Unfolding the Dry Protein. The hypothetical reaction of unfolding the dry protein in a vacuum is represented by similar sums of products; the parameters are given in ref. 3.

$$\begin{aligned}\Delta H_c &= \sum h_{ic} \Delta ASA_i \\ \Delta S_c &= \sum s_{ic} \Delta ASA_i \\ \Delta G_c &= \Delta H_c - T \Delta S_c.\end{aligned}\quad [3]$$

It is not surprising to represent ΔH_c^u in this way, since the change in ASA of a particular group on unfolding is proportional to the number of contact interactions made by the group that are broken on unfolding. It may also be reasonable to represent ΔS_c^u , the increase in conformational entropy on unfolding the dry protein, by this formalism because breaking contact interactions with other groups will increase the freedom of movement of the group. The use of contact area might be better than the use of ASA for the calculation, but it becomes necessary to validate the use of different ΔASA s for the evaluation of unfolding thermodynamics on hydration and dry protein. Furthermore, this introduces other problems. The success or failure of this representation can be assessed from the success of the fitting parameters in predicting thermodynamics for proteins.

Temperature Dependence of Thermodynamics of Unfolding. To predict ΔH^u and ΔS^u for unfolding in aqueous solution as a function of temperature, the first step is to compute these quantities at 25°C by the procedure outlined above. The second step is to compute $\Delta C_{p,h}$ by using the parameters in ref. 2. Next, the assumption is made that $\Delta C_{p,h}$ is independent of temperature and that $\Delta C_{p,c}$ can be neglected (2). Then standard equations can be used to compute the thermodynamics of unfolding as a function of temperature.

$$\begin{aligned}\Delta G^u &= \Delta H^u - T \Delta S^u \\ \Delta H^u(T) &= \Delta H^u(T_0) + \Delta C_{p,h}(T - T_0) \\ \Delta S^u(T) &= \Delta S^u(T_0) + \Delta C_{p,h} \ln(T/T_0).\end{aligned}\quad [4]$$

The reference temperature T_0 is 298.2 K.

ASA. The ASAs of various groups in the protein were computed from the atomic coordinates given in the Protein Data Bank (17). To represent the unfolded protein, an extended polypeptide chain with the known amino acid sequence was generated using backbone dihedral angles of $\phi = -155^\circ$ ($\phi = -75^\circ$ for proline) and $\psi = 160^\circ$ along the main chain, together with appropriate χ angles for the side chains (18). Extended α -helical conformations of an alanine peptide with blocked α -NH₂ and α -COOH groups [*N*-acetyl-*N'*-methyl-(L-Ala)_{*n*}-amide] were generated by using ECEPP to find the low-energy conformation (19). Standard dihedral angles were used: for the helix $\phi = -57^\circ$, $\psi = -47^\circ$, and $\chi = 180^\circ$; for the extended chain, $\phi = -155^\circ$, $\psi = 160^\circ$, and $\chi = 180^\circ$.

RESULTS

Predicted Thermodynamics of Unfolding for Four Proteins. Table 1 compares predicted and observed values of ΔG^u and ΔH^u for 4 proteins not included in the 10 proteins used to derive fitting parameters for ΔH_c^u and ΔS_c^u (3). Inspection of Table 1 shows that agreement between observed and predicted values is similar to that found for the 10 initial proteins. The difference between prediction and experiment for ΔG^u should be compared to the size of ΔG_c^u or ΔG_h^u . For T4 lysozyme the difference between predicted and observed

Table 1. Comparison between predicted (Calc) and experimental (Exp) values of ΔG^u , ΔH^u , and ΔS^u for proteins

| Protein* | NR [†] | ΔG^u , kcal·mol ⁻¹ | | | ΔH^u , kcal·mol ⁻¹ | | | ΔS^u , kcal·mol ⁻¹ ·K ⁻¹ | | |
|----------|-----------------|---------------------------------------|------------------|----------|---------------------------------------|-------------------|----------|--|-----|----------|
| | | Calc | Exp | Δ | Calc | Exp | Δ | Calc | Exp | Δ |
| 4PTI | 58 | 15.8 | 15.0 | 0.8 | 57.7 | 50.5 | 7.2 | 141 | 119 | 22 |
| 1CPV | 108 | 10.1 | 14.7 | -4.6 | 42.6 | 48.5 | -5.9 | 109 | 113 | -4 |
| 5RSA | 124 | 8.2 | 2.1 | 6.1 | 61.2 | 47.0 | 14.2 | 178 | 151 | 27 |
| 2LYZ | 129 | 10.0 | 14.4 | -4.4 | 51.3 | 54.4 | -3.1 | 139 | 134 | 5 |
| 2MBN | 153 | 7.0 | 10.8 | -3.8 | 36.7 | 0.2 | 36.5 | 100 | -36 | 136 |
| 2LZM | 164 | 1.9 | 6.0 | -4.1 | 15.9 | 26.9 | -11.0 | 47 | 70 | -23 |
| 8PAP | 212 | 16.6 | 18.6 | -2.0 | 25.9 | 22.0 | 3.9 | 31 | 11 | 20 |
| 2CAB | 256 | 17.5 | 11.0 | 6.5 | 54.5 | 52.0 | 2.5 | 124 | 137 | -13 |
| 1ABP | 306 | 12.7 | 9.2 | 3.5 | 60.6 | 60.8 | -0.2 | 161 | 173 | -12 |
| 2TAA | 478 | 39.8 | 40.8 | -1.0 | 208.1 | 215.1 | -7.0 | 565 | 585 | -20 |
| 3CYT | 103 | 6.3 | 9.4 [‡] | -3.1 | 21.9 | 16.0 [‡] | 5.9 | 52 | 22 | 30 |
| 1RNT | 104 | 13.8 | 8.7 | 5.1 | 54.4 | 64.7 | -10.3 | 136 | 188 | -52 |
| 2SSI | 214 | 11.5 | 14.4 | -2.9 | 75.9 | 58.2 | 17.7 | 216 | 147 | 69 |
| 4CHA | 239 | 18.2 | 11.2 | 7.0 | 91.7 | 72.0 | 19.7 | 246 | 204 | 42 |

Thermodynamic data for unfolding given for the first 10 proteins were used to derive the fitting parameters (3) employed in predicting thermodynamic quantities. The comparison between predicted and experimental values for the last 4 proteins provides a test of the method. Temperature is 25°C.

*Identified by Protein Data Bank code. Names of the proteins (references to denaturation data are given in parentheses) are L-arabinose-binding protein (1ABP) (20), carp parvalbumin (1CPV) (21), ribonuclease T1 ([Gln²⁵]1RNT; the coordinates were kindly provided by K. Tomita, Osaka University) (22, 23), carbonic anhydrase B (2CAB) (9), hen egg white lysozyme (2LYZ) (24), bacteriophage T4 lysozyme (2LZM) (25), sperm whale myoglobin (2MBN) (14), streptomyces subtilisin inhibitor dimer (2SSI) (26), taka-amylase A (2TAA) (27), albacore tuna cytochrome c (3CYT) (28), α -chymotrypsin (4CHA) (28), bovine trypsin inhibitor (4PTI) (9), ribonuclease A (5RSA) (29, 30), and papain (8PAP) (31).

[†]Number of residues.

[‡]Data are for bovine cytochrome c.

values (-4.1 kcal·mol⁻¹; 1 cal = 4.184 J) is only 1.1% of the magnitude of ΔG_h^u (-358.5 kcal·mol⁻¹) or ΔG_c^u (360.4 kcal·mol⁻¹). Likewise, for T4 lysozyme the difference between the predicted and observed values of ΔH^u (-11.0 kcal·mol⁻¹) is only 1.3% of the magnitude of ΔH_h^u or ΔH_c^u (about 850 kcal·mol⁻¹) (3). Consequently, no better agreement between theory and experiment can be expected using this method and results for the 4 proteins show satisfactory predictions of the unfolding thermodynamics of a protein from its x-ray structure. Since the number of available experimental data is small and specific interactions are not taken into account by this method, a complete analysis of error is quite difficult. Nevertheless, it will be important to make such a study.

Temperature Dependence of the Unfolding Thermodynamics of T4 Lysozyme. Computed and experimental curves of ΔG^u and ΔH^u versus temperature are shown in Fig. 1. At 25°C, the agreement between prediction and experiment is similar to that of other proteins in Table 1. The temperature dependences of ΔH^u or ΔG^u are governed by the values of ΔC_p . It was found earlier (2) that the values of ΔC_p for 12 proteins were approximated closely by predicted values of $\Delta C_{p,h}$ and it was argued that $\Delta C_{p,c}$ should be small. Fig. 1 shows that the experimental temperature dependences of ΔG^u and ΔH^u are predicted fairly well by the predicted values of $\Delta C_{p,h}$. In particular, the existence of cold denaturation near 0°C, which has been demonstrated experimentally for a T4 lysozyme mutant in 3 M guanidinium chloride (15), is indicated.

Gibbs Energy and Enthalpy of Unfolding the L-Alanine Helix. The L-alanine helix presents a particularly challenging system to study by this method. The helix is quite different in appearance from a globular protein. Whereas globular proteins are stabilized chiefly by the classic hydrophobic interaction (7, 8), with hydrophobic side chains buried in the interior of the protein, this is not true of the L-alanine helix. For a long time, it was thought that short L-alanine peptides must not be able to form even partly stable α -helices in water. However, a block of 20 L-alanine residues showed partial α -helix formation at 25°C when stabilized by an attached

block of 20 ionized residues of L-glutamate (32) or L-lysine (33). Moreover, a 16-residue peptide containing 13 L-alanine residues and solubilized by insertion of 3 L-lysine residues showed partial helix formation in water (34). The enthalpy of helix formation has been measured recently (35) for a 50-residue peptide with the formula Ac-Y(AEAAKA)₈F-NH₂.

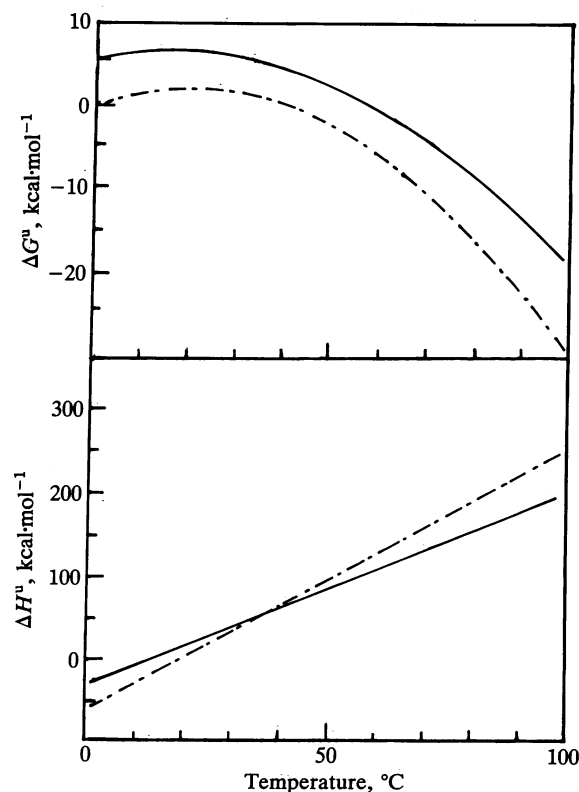


FIG. 1. Computed ΔG^u and ΔH^u (broken lines) for T4 lysozyme are shown as a function of temperature. The experimental curves are given by solid lines.

Table 2. Predicted values for the unfolding thermodynamics of the L-alanine helix

| n | ΔG^u , cal-res ⁻¹ | ΔH^u ($\Delta H_c^u + \Delta H_h^u$), cal-res ⁻¹ | ΔS^u ($\Delta S_c^u + \Delta S_h^u$), cal-res ⁻¹ ·K ⁻¹ | $\Delta C_{p,h}$, cal-res ⁻¹ ·K ⁻¹ |
|-----|---|--|---|--|
| 10 | 2.4 | 630 (2240 – 1610) | 2.1 (4.2 – 2.1) | 1.7 |
| 20 | 1.0 | 780 (2470 – 1690) | 2.6 (4.8 – 2.2) | 1.9 |
| 30 | 0.7 | 830 (2540 – 1710) | 2.8 (5.0 – 2.2) | 1.9 |
| 40 | 0.3 | 860 (2580 – 1720) | 2.9 (5.1 – 2.2) | 2.0 |

The values per mol of residue (res⁻¹) are given. The peptide is Ac(Ala)_nNHMe, where n is the number of alanine residues. Enthalpy and entropy contributions from hydration (h) and chain folding (c) are shown in parentheses. The temperature is 25°C.

The same method used to predict the unfolding thermodynamics of four proteins in Table 1 can be used without change to predict the unfolding thermodynamics of the L-alanine helix. Predicted results are shown in Table 2 for four chain lengths: $n = 10, 20, 30,$ and 40 residues. The values of ΔH^u , ΔS^u , and $\Delta C_{p,h}$ are given per residue. At about $n = 30$, the values change slowly with chain length and may be approaching chain-length-independent limits. The predicted value of ΔH^u (0.86 kcal·res⁻¹) is smaller than reported for the 50-residue alanine-rich peptide [$\Delta H^u = 1.2$ kcal·res⁻¹ (35)], but experimental uncertainty in the measured value is large because the breadth of the unfolding transition curve makes it difficult to place the baseline accurately (35). Similarly, the predicted value of $\Delta C_{p,h}$ (2.0 cal·res⁻¹·K⁻¹) cannot be compared with a measured value because the breadth of the transition curve precludes measurement of ΔC_p (35).

DISCUSSION

Properties of the Method. From its nature, the new method cannot predict thermodynamic properties of proteins that are based on specific interactions, because specific interactions are not treated in this method. Known examples of specific interactions in proteins are electrostatic. In barnase, the ΔG for interaction between a charged histidine near the C terminus of a helix and the α -helix dipole is about -2 kcal (36). In T4 lysozyme, a partly buried ion pair stabilizes the protein by more than -3 kcal (37). Specific interactions like these are included in step 3 of our cycle. Consequently, if specific interactions account for part of the stability of a protein and this protein is included in the data base, then these interactions will contribute to the data base values of ΔH_c^u and ΔS_c^u from which the fitting parameters were obtained (3). This is a source of error in our method and is a basic reason why agreement between the predicted and observed values of ΔG^u and ΔH^u in Table 1 cannot be expected to be better than it is. What is remarkable is that the formalism and fitting parameters of the method are as successful as indicated by the results for the four proteins in Table 1.

The ability of this method to predict the temperature dependences of ΔG^u and ΔH^u rests primarily on the success of approximating ΔC_p by $\Delta C_{p,h}$ and of accurately predicting $\Delta C_{p,h}$ by the formalism of the method. It has been shown (13) that the ratio of ΔC_p to nonpolar ΔASA is the same for protein unfolding and for the transfer of liquid hydrocarbons from neat hydrocarbon to aqueous solution. This result supports our approximation of ΔC_p by $\Delta C_{p,h}$.

The negative values of ΔH_h^u (2, 3) show that the net interaction of dry protein [either N(g) or R(g)] with water is favorable and that the more extensive interaction of water with R(g) favors unfolding. This result, of course, has been surmised from experimental studies of the adsorption of water to dry proteins (38). The sign of ΔH_h^u emphasizes the energetic importance of the interaction with water of polar groups in proteins. An important feature of the method is that it takes into account the burial of peptide NH and CO groups that occurs during protein folding.

Unfolding Thermodynamics of the L-Alanine Helix. Although the L-alanine helix has a quite different structure than that of a typical globular protein, which has buried hydrophobic side chains in its interior, nevertheless both show similar agreement between predicted and observed unfolding thermodynamics (Tables 1 and 2). Since the fitting parameters for step 3 of our cycle are derived from a data base of 10 globular proteins, this is a remarkable result. It is very encouraging that the same set of fitting parameters used to reproduce the unfolding thermodynamics of globular proteins can predict the enthalpy change for formation of the L-alanine helix.

It is interesting to examine the end effect on helix stability predicted by this method. The 10-residue peptide forms an enthalpically less stable helix (per residue) than a 40-residue peptide, as might be expected for the deficit of hydrogen bonds at each end of the helix (three hydrogen bonds at the N-terminal end if the acetyl group can hydrogen bond; four hydrogen bonds at the C-terminal end), but this effect is slightly more than offset by the smaller decrease in entropy per residue in the 10-residue helix. Although this method is not able to predict the magnitude of the helix nucleation constant σ , it does suggest the nature of the enthalpic and entropic contributions to σ for L-alanine helix formation in water.

The main results in Table 2 are that the L-alanine helix is predicted to have partial helix stability in water and that helix formation is enthalpy-driven. The latter prediction has been confirmed by experiment, both by thermal unfolding curves measured by circular dichroism (32–34) and recently by direct calorimetric measurement of ΔH^u (35) for a 50-residue alanine-rich helix. The predicted value of $\Delta G^u/RT$ per residue is close to 0 and so the Zimm–Bragg parameter s is close to 1, in agreement with host–guest measurements of s for L-alanine (39). The experimental situation is not clear, however, because short alanine peptides show partial helix formation in water (32–34), in contrast to prediction based on the Zimm–Bragg equation using host–guest parameters for L-alanine.

We sincerely thank Prof. R. L. Baldwin for valuable suggestions and advice in completing the manuscript. This work was supported in part by research grants from the Ministry of Education, Science, and Culture of Japan and Kyoto Women's University.

- Ooi, T., Oobatake, M., Némethy, G. & Scheraga, H. A. (1987) *Proc. Natl. Acad. Sci. USA* **84**, 3086–3090.
- Ooi, T. & Oobatake, M. (1988) *J. Biochem. (Tokyo)* **103**, 114–120.
- Ooi, T. & Oobatake, M. (1988) *J. Biochem. (Tokyo)* **104**, 440–444.
- Ooi, T. & Oobatake, M. (1988) *Comments Mol. Cell. Biophys.* **5**, 233–251.
- Khechinashvili, N. N. (1990) *Biochim. Biophys. Acta* **1040**, 346–354.
- Cabani, S., Gianni, P., Mollica, V. & Lepori, L. (1981) *J. Solution Chem.* **10**, 563–595.
- Kauzmann, W. (1959) *Adv. Protein Chem.* **14**, 1–63.
- Nozaki, Y. & Tanford, C. (1971) *J. Biol. Chem.* **246**, 2211–2217.
- Privalov, P. L. (1979) *Adv. Protein Chem.* **33**, 167–241.

10. Sturtevant, J. M. (1977) *Proc. Natl. Acad. Sci. USA* **74**, 2236–2240.
11. Baldwin, R. L. (1986) *Proc. Natl. Acad. Sci. USA* **83**, 8069–8072.
12. Becktel, W. J. & Schellman, J. A. (1987) *Biopolymers* **26**, 1859–1877.
13. Spolar, R. S., Ha, J.-H. & Record, M. T., Jr. (1989) *Proc. Natl. Acad. Sci. USA* **86**, 8382–8385.
14. Privalov, P. L., Griko, Y. V., Venyaminov, S. Y. & Kutysenko, V. P. (1986) *J. Mol. Biol.* **190**, 487–498.
15. Chen, B. & Schellman, J. A. (1989) *Biochemistry* **28**, 685–691.
16. Shrake, A. & Rupley, J. A. (1973) *J. Mol. Biol.* **79**, 351–371.
17. Bernstein, F. C., Koetzle, T. F., Williams, G. J. B., Meyer, E. F., Jr., Brice, M. D., Rodgers, J. R., Kennard, O., Shimanouchi, T. & Tasumi, M. (1977) *J. Mol. Biol.* **112**, 535–542.
18. Oobatake, M. & Ooi, T. (1989) *Bull. Inst. Chem. Res. Kyoto Univ.* **66**, 433–445.
19. Némethy, G., Pottle, M. S. & Scheraga, H. A. (1983) *J. Phys. Chem.* **87**, 1883–1887.
20. Fukada, H., Sturtevant, J. M. & Quijcho, F. A. (1983) *J. Biol. Chem.* **258**, 13193–13198.
21. Filimonov, V. V., Pfeil, W., Tsalkova, T. N. & Privalov, P. L. (1987) *Biophys. Chem.* **8**, 117–122.
22. Oobatake, M., Takahashi, S. & Ooi, T. (1979) *J. Biochem. (Tokyo)* **86**, 55–63.
23. Pace, C. N. & Laurents, D. V. (1989) *Biochemistry* **28**, 2520–2525.
24. Pfeil, W. & Privalov, P. L. (1976) *Biophys. Chem.* **4**, 41–50.
25. Hawkes, R., Grutter, M. G. & Schellman, J. A. (1984) *J. Mol. Biol.* **175**, 195–212.
26. Takahashi, K. & Sturtevant, J. M. (1981) *Biochemistry* **20**, 6185–6190.
27. Fukada, H., Takahashi, K. & Sturtevant, J. M. (1987) *Biochemistry* **26**, 4063–4068.
28. Privalov, P. L. & Khechinashvili, N. N. (1974) *J. Mol. Biol.* **86**, 665–684.
29. Brandts, J. F. & Hunt, L. (1967) *J. Am. Chem. Soc.* **89**, 4826–4838.
30. Tsong, T. Y., Hearn, R. P., Wrathall, D. P. & Sturtevant, J. M. (1970) *Biochemistry* **9**, 2666–2677.
31. Tiktopulo, E. I. & Privalov, P. L. (1978) *FEBS Lett.* **91**, 57–58.
32. Ihara, S., Ooi, T. & Takahashi, S. (1982) *Biopolymers* **21**, 131–145.
33. Takahashi, S., Kim, E.-H., Hibino, T. & Ooi, T. (1989) *Biopolymers* **28**, 995–1009.
34. Marqusee, S., Robbins, V. H. & Baldwin, R. L. (1989) *Proc. Natl. Acad. Sci. USA* **86**, 5286–5290.
35. Scholtz, J. M., Marqusee, S., Baldwin, R. L., York, E. J., Stewart, J. M., Santoro, M. & Bolen, D. W. (1991) *Proc. Natl. Acad. Sci. USA* **88**, 2854–2858.
36. Sali, D., Byroft, M. & Fersht, A. R. (1988) *Nature (London)* **335**, 740–743.
37. Anderson, D. E., Becktel, W. J. & Dahlquist, F. W. (1990) *Biochemistry* **29**, 2403–2408.
38. Rupley, J. A., Gratton, E. & Careri, G. (1983) *Trends Biochem. Sci.* **8**, 18–22.
39. Platzer, K. E. B., Ananthanarayanan, V. S., Andreatta, R. H. & Scheraga, H. A. (1972) *Macromolecules* **5**, 177–187.